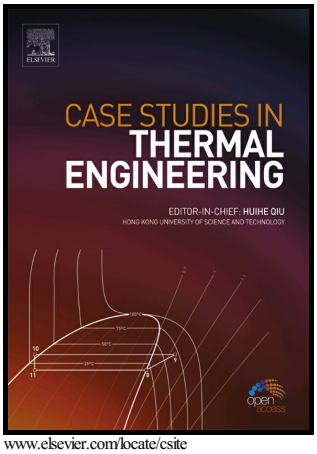

www.elsevier.com/locate/csite

Magneto-Marangoni nano-boundary layer flow of water and ethylene glycol based γ Al_2O_3 nanofluids with non-linear thermal radiation effects

N. Vishnu Ganesh, Ali J. Chamkha, Qasem M. Al-Mdallal, P.K. Kameswaran

PII: S2214-157X(18)30083-2
DOI: https://doi.org/10.1016/j.csite.2018.04.019
Reference: CSITE290

To appear in: *Case Studies in Thermal Engineering*

Received date: 29 March 2018
Revised date: 13 April 2018
Accepted date: 29 April 2018

Cite this article as: N. Vishnu Ganesh, Ali J. Chamkha, Qasem M. Al-Mdallal and P.K. Kameswaran, Magneto-Marangoni nano-boundary layer flow of water and ethylene glycol based γ Al_2O_3 nanofluids with non-linear thermal radiation effects, *Case Studies in Thermal Engineering,* https://doi.org/10.1016/j.csite.2018.04.019

Magneto-Marangoni nano-boundary layer flow of water and ethylene glycol based γ Al_2O_3 nanofluids with non-linear thermal radiation effects

N. Vishnu Ganesh[a], ,Ali J. Chamkha[b,c], Qasem M. Al-Mdallal[d], P.K. Kameswaran[e]

[a] Department of Mathematics, Ramakrishna Mission Vivekananda College, Mylapore, Chennai - 600004, Tamil Nadu, INDIA.

[b] Mechanical Engineering Department, Prince Sultan Endowment for Energy and Environment, Prince Mohammad Bin Fahd University, Al-Khobar 31952, Saudi Arabia.

[c] RAK Research and Innovation Center, American University of Ras Al Khaimah, P.O. Box 10021, Ras Al Khaimah, United Arab Emirates.

[d] Department of Mathematical Sciences, United Arab Emirates University, P.O. Box 15551, Al Ain, Abu Dhabi, United Arab Emirates.

[e] Department of Mathematics, VIT University, Vellore, Tamil Nadu, India

corresponding author email: ntpvishnuganesh@rmv.ac.in

Abstract

For the first time, a numerical investigation is performed to study the influences of magnetic field on Marangoni boundary layer flow of water and ethylene glycol based γ Al_2O_3 nanofluids over a flat surface in the presence of non–linear thermal radiation. Experimental based thermo-physical properties and an effective Prandtl number model for γ Al_2O_3 nanofluids are considered to analyse the Marangoni convection. To study the magnetic field effects, the electric conductivities of both nanoparticles and base fluids are taking into account. Numerical solutions of resulted equations are obtained using fourth order Runge-Kutta method with shooting technique. The combined effect of magnetic parameter with other involved parameters is discussed on velocity and temperature distributions and the local Nusselt number via graphical illustrations.

Keywords: Effective Prandtl number; Magnetic field; Marangoni boundary layer; γ-Al_2O_3 nanoparticles; non-linear radiation;

Nomenclature

B_0	magnetic field strength (Tesla)	σ_0	the surface tension at the interface (N/m)
k^*	mean absorption coefficient (m^{-1})	$\overline{\sigma}$	rate of change of surface tension with temperature
M_n	magnetic parameter (-)	σ_{nf}	the electric conductivity of the nanofluid (S m^{-1})
k_{nf}	thermal conductivity of the nanofluid (W/m.K)	σ_s	the electric conductivity of the nanoparticles (S m^{-1})
k_f	thermal conductivity of the base fluid (W/m.K)	σ_f	the electric conductivity of the base fluid (S m^{-1})
Pr_{nf}	Prandtl number of nanofluid (-)	σ^*	Stefan- Boltzman constant (-)
Pr_f	Prandtl number of base fluid (-)	ϕ	solid volume fraction of nanofluid (-)
q_r	Radiative heat flux (W/m^2)	μ_{nf}	effective dynamics viscosity of the nanofluid (N. s/ m^2)
		μ_f	Dynamics viscosity of the base fluid(N. s/ m^2)
R_d	radiation parameter (-)	ρ_{nf}	the effective density of the nanofluid (kg m^{-3})
Nu_x	local Nusselt number (-)	ρ_s	density of the base fluid (kg m^{-3})
T	local temperature of the fluid (K)	ρ_f	density of the nanoparticles(kg m^{-3})
T_w	temperature at the wall (K)	θ	dimensionless temperature (-)
T_∞	ambient temperature (K)	θ_w	temperature ratio parameter (-)
u, v	velocity components in *x* and *y* directions (m s^{-1})	η	space variable (-)
x, y	coordinates along and perpendicular to the surface (m)		

1. Introduction

In recent years, magneto-Marangoni convection has become a popular research topic because of its various applications in many engineering fields such as mechanical, aerospace, chemical engineering, crystal growth processing, thin liquid films, materials science engineering and so on. The magneto-Marangoni convection of nanofluids can be defined as interfacial electrically conducting nanoliquid flow driven by the surface tension gradient under the influence of magnetic field.

Many attentions have been taken to study the heat transfer characteristics of different types of nanofluids and one can get clear and brief introduction and applications about nanofluids in the following publications [1-22]. Recently, both theoretical and experimental

researchers have turned their interest to study the γ Al_2O_3 nanofluids because of its applications in cooling processes [23-32]. Very recently, Moghaieb et al. [33] used γ Al_2O_3-H_2O nanofluid as an engine coolant in their study. A comparative study of Al_2O_3 and γ Al_2O_3 nanofluids over a stretching sheet has been conducted by Vishnu Ganesh et al. [34]. Rashidi et al. [35] studied the effects of an effective Prandtl number model on the boundary layer flow of γ Al_2O_3-H_2O and γ Al_2O_3- $C_2H_6O_2$ over a vertical stretching sheet. Recently, the Marangoni boundary layer flow of nanofluid has been discussed with various physical effects using well known thermo-physical properties model for base fluid and nanoparticles without any effective Prandtl number [36-40].

No attempt has been made to study the magneto-Marangoni boundary layer flow of water and ethylene glycol based γ Al_2O_3 nanofluids with nonlinear thermal radiation effects. Experimental based thermo-physical properties and an effective Prandtl number model for γ Al_2O_3 nanofluids are considered to analyse the Marangoni convection. The electric conductivities of both nanoparticles and base fluids are taking into account to study the magnetic field effects.

2. **Formulation of the Problem**

Consider the steady two-dimensional incompressible Marangoni boundary layer flow over a flat surface in a water/ethylene glycol based nanofluid containing γ Al_2O_3 nanoparticles in the presence of non-linear thermal radiation. It is assumed that the flow is laminar and the base fluid and the nanoparticles are in thermal equilibrium. A constant magnetic field strength of B_0 is applied in the transverse direction and also the external electric field is assumed to be zero and the magnetic Reynolds number is assumed to be small (The induced magnetic field is negligible compared to applied magnetic field). The thermo-physical properties are considered as given in Table.1. We consider the a Cartesian coordinate system (x,y), where x and y are the coordinates measured along the stretching

sheet and normal to it. The flow takes place at $y \geq 0$. In addition, T_w and T_∞ are the temperature of the surface and ambient fluid, respectively.

Furthermore, it is assumed that the surface tension σ is vary linearly with temperature as [37]:

$$\sigma = \sigma_0 \left[1 - \overline{\sigma}\left(T - T_\infty\right)\right] \tag{1}$$

where σ_0 is the surface tension at the interface and $\overline{\sigma}$ is the rate of change of surface tension with temperature.

Taking the above assumptions into consideration, the steady boundary layer equations governing the convective flow and heat transfer for a nanofluid in the presence of magnetic field and thermal radiation can be written as **[6, 34, 35]**

$$\frac{\partial u}{\partial x} + \frac{\partial v}{\partial y} = 0, \tag{2}$$

$$u\frac{\partial u}{\partial x} + v\frac{\partial u}{\partial y} = \frac{\mu_{nf}}{\rho_{nf}}\frac{\partial^2 u}{\partial y^2} - \frac{\sigma_{nf}\, B_0^2\, u}{\rho_{nf}}, \tag{3}$$

$$u\frac{\partial T}{\partial x} + v\frac{\partial T}{\partial y} = \frac{k_{nf}}{\left(\rho C_p\right)_{nf}}\frac{\partial^2 T}{\partial y^2} - \frac{1}{\left(\rho C_p\right)_{nf}}\left(\frac{\partial q_r}{\partial y}\right). \tag{4}$$

The corresponding boundary conditions are

$$v = 0, \qquad T = T_\infty + bx^2, \qquad \mu_{nf}\left(\frac{\partial u}{\partial y}\right) = \frac{\partial \sigma}{\partial T}\frac{\partial T}{\partial x} \qquad \text{at} \qquad y = 0,$$

$$u \to 0, \qquad T \to T_\infty \qquad \text{as} \qquad y \to \infty, \tag{5}$$

where u and v are the velocity components along the axis x and y, respectively, T is the temperature of the nanofluid, T_∞ is the temperature of the nanofluid far away from the wall, σ_{nf} is the electric conductivity of the nanofluid and q_r is the radiative heat flux.

Using the Rosseland approximation for non-linear thermal radiation, the radiative heat flux is given by **[22]**

$$q_r = -\frac{4\sigma^*}{3k^*}\frac{\partial T^4}{\partial y} = -\frac{16\sigma^*}{3k^*}T^3\frac{\partial T}{\partial y} \tag{6}$$

where σ^* and k^* are the Stefan- Boltzman constant and the mean absorption coefficient, respectively. Now Eq. (4) can be expressed as

$$u\frac{\partial T}{\partial x} + v\frac{\partial T}{\partial y} = \frac{\partial}{\partial y}\left[\left(\frac{k_{nf}}{(\rho C_p)_{nf}} + \frac{16\sigma^* T^3}{3(\rho C_p)_{nf}k^*}\right)\frac{\partial T}{\partial y}\right]. \tag{7}$$

3. Thermo-physical Properties of γ Al_2O_3-H_2O and γ Al_2O_3- $C_2H_6O_2$ Nanofluids

The effective dynamic density (ρ_{nf}), the heat capacitance ($(\rho C_p)_{nf}$) and the electric conductivity (σ_{nf}) of the nanofluid are defined as

$$\rho_{nf} = (1-\phi)\rho_f + \phi\rho_s, \qquad (\rho C_p)_{nf} = (1-\phi)(\rho C_p)_f + \phi(\rho C_p)_s,$$

$$\frac{\sigma_{nf}}{\sigma_f} = \left[1 + \frac{3\left(\frac{\sigma_s}{\sigma_f} - 1\right)\phi}{\left(\frac{\sigma_s}{\sigma_f} + 2\right) - \left(\frac{\sigma_s}{\sigma_f} - 1\right)\phi}\right] \tag{8}$$

where ϕ is the solid volume fraction of nanofluid.

The dynamic viscosity of $\gamma\, Al_2O_3$ nanofluids is given by **[23-25]**

$$\frac{\mu_{nf}}{\mu_f} = 123\phi^2 + 7.3\,\phi + 1, \qquad \text{(for } \gamma\, Al_2O_3\text{-}H_2O\text{)}, \tag{9}$$

$$\frac{\mu_{nf}}{\mu_f} = 306\phi^2 - 0.19\,\phi + 1, \qquad \text{(for } \gamma\, Al_2O_3\text{-}\, C_2H_6O_2\ \text{)}. \tag{10}$$

The effective thermal conductivity of $\gamma\, Al_2O_3$ nanofluids is given **by [23-25]**

$$\frac{k_{nf}}{k_f} = 4.97\phi^2 + 2.72\,\phi + 1, \qquad \text{(for } \gamma\, Al_2O_3\text{-}H_2O\text{)}, \tag{11}$$

$$\frac{k_{nf}}{k_f} = 28.905\phi^2 + 2.8273\,\phi + 1, \qquad \text{(for } \gamma\, Al_2O_3\text{-}\, C_2H_6O_2\ \text{)}. \tag{12}$$

The effective Prandtl number of $\gamma\, Al_2O_3$ nanofluids is given by **[26]**

$$\frac{\mathrm{Pr}_{nf}}{\mathrm{Pr}_f} = 82.1\phi^2 + 3.9\,\phi + 1, \qquad \text{(for } \gamma\, Al_2O_3\text{-}H_2O\text{)}, \tag{13}$$

$$\frac{\mathrm{Pr}_{nf}}{\mathrm{Pr}_f} = 254.3\phi^2 - 3\,\phi + 1, \qquad \text{(for } \gamma\, Al_2O_3\text{-}\, C_2H_6O_2\ \text{)}. \tag{14}$$

Equation (8) is the general relationship used to calculate the density, specific heat and electric conductivity for nanofluids. Eqs. (9) and (10) are the dynamic viscosity of nanofluids that have been obtained by performing a least-square curve fitting of some scarce experimental data available for the mixtures considered [41-43]. It has been found that these formulas considerably underestimate the viscosity of the $\gamma\, Al_2O_3$ nanofluids under consideration with respect to the measured experimental data as shown by Maiga et al. [23]. Eqs. (11) and (12) are obtained from the well-known model proposed by Hamilton and Crosser [44], regarding the thermal conductivity of the nanofluids, the same situation does

exist for $\gamma\ Al_2O_3$ nanofluids [23]. Eqs. (13) and (14) are the effective Prandtl number of $\gamma\ Al_2O_3$ nanofluids which are obtained by a curve fitting using regression laws [26].

4. Similarity Transformations and Non-dimensionalization

By using the following non- dimensional variables [37]

$$\psi(\eta) = \xi_2\, x\, f(\eta), \qquad \theta = \frac{T - T_\infty}{T_w - T_\infty}, \qquad \eta = \xi_1\, y \tag{15}$$

where $\xi_1 = \left(\dfrac{\sigma_0\, \bar{\sigma}\, a\, \rho_f}{\mu_f{}^2} \right)^{1/3}$, $\xi_2 = \left(\dfrac{\sigma_0 \bar{\sigma}\, a\, \mu_f}{\rho_f{}^2} \right)^{1/3}$,

the governing boundary layer equations (3) and (7) are transformed to non-dimensional ordinary differential equations as follow:

4.1. Momentum equation

$$f''' + \frac{1}{\left(123\phi^2 + 7.3\,\phi + 1\right)} \left[\left(1 - \phi + \phi \left(\frac{\rho_s}{\rho_f} \right) \right) \left(f\, f'' - f'^{\,2} \right) - \left[1 + \frac{3\left(\dfrac{\sigma_s}{\sigma_f} - 1 \right)\phi}{\left(\dfrac{\sigma_s}{\sigma_f} + 2 \right) - \left(\dfrac{\sigma_s}{\sigma_f} - 1 \right)\phi} \right] Mn\, f' \right] = 0$$

(for $\gamma\ Al_2O_3$-H_2O),

$$f''' + \frac{1}{(306\phi^2 - 0.19\,\phi + 1)} \left[\left(1 - \phi + \phi \left(\frac{\rho_s}{\rho_f} \right) \right) \left(f\, f'' - f'^{\,2} \right) - \left[1 + \frac{3\left(\dfrac{\sigma_s}{\sigma_f} - 1 \right)\phi}{\left(\dfrac{\sigma_s}{\sigma_f} + 2 \right) - \left(\dfrac{\sigma_s}{\sigma_f} - 1 \right)\phi} \right] Mn\, f' \right] = 0$$

(for $\gamma\ \ Al_2O_3$- $C_2H_6O_2$).

(16)

4.2. Energy Equation

$$\theta''\left[1+R_d\,A\left(\theta\left(\theta_w-1\right)+1\right)^3\right]+R_d\,A\left[3\theta'^2\left(\theta_w-1\right)\left(\theta\left(\theta_w-1\right)+1\right)^2\right]+B\left(f\,\theta'-2\theta\,f'\right)=0, \tag{17}$$

where

$$A=\left(4.97\,\phi^2+2.72\,\phi+1\right)^{-1} \quad \text{and} \quad B=\frac{\mathrm{Pr}_f\left(1-\phi+\phi\left(\frac{\rho_s}{\rho_f}\right)\right)\left(82.1\phi^2+3.9\,\phi+1\right)}{123\phi^2+7.3\,\phi+1}$$

(for γ Al_2O_3-H_2O),

$$A=\left(28.905\phi^2+2.8273\,\phi+1\right)^{-1} \quad \text{and} \quad B=\frac{\mathrm{Pr}_f\left(1-\phi+\phi\left(\frac{\rho_s}{\rho_f}\right)\right)\left(254.3\phi^2-3\,\phi+1\right)}{306\phi^2-0.19\,\phi+1}$$

(for γ Al_2O_3- $C_2H_6O_2$),

The corresponding boundary conditions are

$$f(0)=0, \qquad f''(0)=\frac{-2}{C}, \qquad f'(\infty)=0$$

$$\theta(0)=1 \qquad \text{and} \qquad \theta(\infty)=0. \tag{18}$$

where

$C=123\,\phi^2+7.3\,\phi+1$ (for γ Al_2O_3-H_2O),

$C=306\,\phi^2-0.19\,\phi+1$ (for γ Al_2O_3- $C_2H_6O_2$), $Mn=\frac{\sigma_f\,B_0^2}{\rho_f\,\xi_1\,\xi_2}$ is the magnetic parameter, $R_d=\frac{16\sigma^*T_\infty^3}{3k^*k_f}$ is the radiation parameter and $\theta_w=\frac{T_w}{T_\infty}$ is the temperature ratio parameter.

The surface velocity is defined as

$$u_w = \left[\frac{\left(\sigma_0 \bar{\sigma} a\right)^2}{\rho_f \mu_f} \right]^{1/3} x f'(0).$$

The local Nusselt number Nu_x can be defined as

$$Nu_x = \frac{x q_w}{k_f (T_w - T_\infty)}, \tag{19}$$

where $q_w = -k_{nf}\left(\frac{\partial T}{\partial y}\right)_{y=0} + (q_r)_w$ is the local surface heat flux.

Using (15), we obtain the following Nusselt number

$$Nu_x = D\,\theta'(0)\xi_1\, x \tag{20}$$

Where

$$D = -\left(4.97\phi^2 + 2.72\,\phi + 1\right)\left[1 + \frac{R_d(\theta_w)^3}{\left(4.97\phi^2 + 2.72\,\phi + 1\right)}\right] \text{(for } \gamma\, Al_2O_3\text{-}H_2O\text{) and}$$

$$D = -\left(28.905\phi^2 + 2.8273\,\phi + 1\right)\left[1 + \frac{R_d(\theta_w)^3}{\left(28.905\phi^2 + 2.8273\,\phi + 1\right)}\right] \text{(for } \gamma\, Al_2O_3\text{- } C_2H_6O_2\text{),}$$

5. Numerical Technique

The governing non- dimensionless ODEs ((16) and (17) subject to the BC's (18) have been solved numerically by fourth order RK method with shooting technique. The governing equations have been reduced into a set of first order ODEs.

$$\begin{bmatrix} y_1' \\ y_2' \\ y_3' \\ y_4' \\ y_5' \end{bmatrix} = \begin{bmatrix} y_2 \\ y_3 \\ -C^{-1}\left[\left(1-\phi+\phi\left(\frac{\rho_s}{\rho_f}\right)\right)\left(y_1 y_3 - y_2^2\right) - \left[1+\frac{3\left(\frac{\sigma_s}{\sigma_f}-1\right)\phi}{\left(\frac{\sigma_s}{\sigma_f}+2\right)-\left(\frac{\sigma_s}{\sigma_f}-1\right)\phi}\right] Mn\ y_2\right] \\ y_4' \\ \frac{-R_d A\left[3y_5^2(\theta_w-1)\left(y_4(\theta_w-1)+1\right)^2\right] - B\left[y_1 y_5 - 2 y_4 y_2\right]}{1+R_d A\left[y_4(\theta_w-1)+1\right]^3} \end{bmatrix} \quad \textbf{(21)}$$

and the corresponding initial conditions are:

$$\begin{bmatrix} y_1 \\ y_2 \\ y_3 \\ y_4 \\ y_5 \end{bmatrix} = \begin{bmatrix} 0 \\ g_1 \\ -2/C \\ 1 \\ g_2 \end{bmatrix} \quad \textbf{(22)}$$

First order Equations in (21) with initial conditions (22) are solved using fourth order Runge–Kutta integration technique. Suitable guessing values of the unknown initial conditions g_1 and g_2 are approximated by shooting method until the boundary conditions at $f'(\infty)=0$ and $\theta(\infty)=0$ are satisfied with the accuracy of 10^{-6}.

6. Results and Discussion

The numerical results of non-dimensional velocity profile, non-dimensional temperature profile and reduced Nusselt number are obtained by above explained numerical method. The results are plotted to show the combined effect of magnetic parameter and other pertinent physical parameters on the flow of water and ethylene glycol based γ Al_2O_3 nanofluids. The velocity and temperature profiles of nanofluid are discussed for two cases, namely in the presence of magnetic field (*Mn* = 0) and in the absence of magnetic field (*Mn*=

Positive number). The Prandtl number of water and ethylene glycol is fixed as 6.96 and 204 respectively.

The magnetic parameter *Mn* is a key parameter to understand the flow behaviour of the nanofluid under the influence of magnetic field. The combined effects of magnetic parameter and the nanoparticle volume fraction of γAl_2O_3 nanofluids on the Marangoni velocity profile are shown in Figs 1(a) and 1(b). It is noted that, an increment in the nanoparticle volume fraction accelerates the velocity profile far away from the wall of the surface and decelerates the velocity profile near the wall of the surface. It is also noted that the velocity profile of both water and ethylene glycol based γ Al_2O_3 nanofluids decreases in the presence of magnetic field and increases in the absence of magnetic field. This is due to the fact that the presence of magnetic field leads to produce a resistive type force (Lorentz force) in the flow region, which arrests the motion of the fluid. The combined effect of magnetic and nanoparticle volume fraction parameters decrease the thickness of the nano-momentum boundary layer. On comparing these figures, the nano-momentum boundary layer thickness of ethylene glycol based nanofluid is higher than the thickness of the nano-momentum boundary layer of water based nanofluid.

The combined effects of magnetic parameter and the nanoparticle volume fraction of γ Al_2O_3 nanofluids on the Marangoni temperature profile are elucidated in Figs. 2(a) and 2(b). It is noted that an increment in the nanoparticle volume fraction diminishes the temperature profile. It is also observed that the temperature profile of both water and ethylene glycol based γ Al_2O_3 nanofluids enhances in the presence of magnetic field and diminishes in the absence of magnetic field. The combined effects of magnetic and nanoparticle volume fraction parameters increase the thickness of the nano-thermal boundary layer. On comparing these figures, the nano-thermal boundary layer thickness of water based nanofluid is higher than the thickness of the nano-thermal boundary layer of the ethylene glycol based nanofluid.

Fig. 3(a) and 3(b) demonstrate the combined effect of magnetic and the radiation parameters in the Marangoni temperature profile of water and ethylene glycol based γ Al_2O_3 nanofluids, respectively. It is clear that the temperature profile of the nanofluid increases as radiation parameter increases. The absorption coefficient decreases whenever radiation parameter increases. This fact leads to increase the temperature profile of both the nanofluids. The combined effects of magnetic and the radiation parameters lead to increase the thickness of the nano-thermal boundary layer.

The variation of local Nusslelt number with physical parameters displayed in the Figs. 4 and 5. The magnetic parameter and the reduced Nusslet number are chosen as *x* and *y* axes respectively. From these figures, It is seen that the magnitude of local Nusselt number decreases with magnetic parameter and increase with nanoparticle volume fraction, radiation and temperature ratio parameters. On comparing the figures 4(a), 4(b), 5(a) and 5(b), it is clear that the magnitude reduced Nusselt number of ethylene glycol based γ Al_2O_3 nanofluid is higher than that of water based γ Al_2O_3 nanofluid.

7. Conclusion

Marangoni boundary layer flow of water and ethylene glycol based γ Al_2O_3 nanofluids under the influence of constant magnetic field and non-linear thermal radiation is investigated. The governing non- dimensional equations are solved numerically. The following significant results are noticed.

- The nanoparticle volume fraction parameter decelerates velocity profile near the wall of the surface and accelerates the velocity profile far away from the wall of the surface. The temperature profile diminishes with nanoparticle volume fraction.

- The combined effect of magnetic and nanoparticle volume fraction parameters decrease the thickness of the nano-momentum boundary layer and increase the thickness of the nano-thermal boundary layer. The combined effects of magnetic and the radiation parameters lead to increase the thickness of the nano-thermal boundary layer.
- The nano-momentum boundary layer thickness of ethylene glycol-based γ Al_2O_3 nanofluid is higher than the thickness of the nano-momentum boundary layer of the water based γ Al_2O_3 nanofluid and an opposite phenomenon has been observed in nano-thermal boundary layer thickness.
- The local Nusselt number decreases with magnetic parameter and increases with nanoparticle volume fraction, radiation and temperature ratio parameters.

Acknowledgment

The authors wish to express their sincere thanks to the honourable referees for their valuable comments and suggestions to improve the quality of the paper. Authors would like to acknowledge and express their gratitude to the United Arab Emirates University, Al Ain, UAE for providing the financial support with Grant No. 31S240-UPAR (2) 2016.

References

[1] S.U.S. Choi, Enhancing thermal conductivity of fluids with nanoparticles, Developments and Applications of Non-Newtonian Flows, FED-vol. 231/MDvol. 66 (1995) 99-105

[2] K. Vajravelu, K.V. Prasad, Jinho Lee, Changhoon Lee, I.Pop, A.Robert Van Gorder, Convective heat transfer in the flow of viscous Ag-water and Cu- water nanofluids over a stretching surface, Int. J. Thermal Sciences, 50 (2011) 843-851.

[3] M. Turkyilmazoglu, Exact analytical solutions for heat and mass transfer of MHD slip flow in nanofluids, Chem. Eng. Sci., 84 (2012) 182-187.

[4] P.K. Kameswaran, M. Narayana, P. Sibanda, P.V.S.N. Murthy, Hydromagnetic nanofluid flow due to a stretching or shrinking sheet with viscous dissipation and chemical reaction effects, Int. J. Heat and Mass Transfer, 55 (2012) 7587-7595.

[5] P.K. Kameswaran, S. Shaw, P. Sibanda, P.V.S.N. Murthy, Homogeneous-heterogeneous reactions in a nanofluid flow due to a porous stretching sheet, Int. J. Heat and Mass Transfer, 57 (2013) 465-472.

[6] M. Fakour, A. Vahabzadeh, D.D.Ganji, Scrutiny of mixed convection flow of a nanofluid in a vertical channel, Case Studies in Thermal Engineering, 4 (2014) 15-23.

[7] M.M. Rashidi, A. Hosseini, I. Pop, S. Kumar, N. Freidoonimehr, Comparative numerical study of single and two-phase models of nanofluid heat transfer in wavy channel, Applied Mathematics and Mechanics., 35(7) (2014) 831-848 (2014)

[8] A.K. Abdul Hakeem, N. Vishnu Ganesh, B. Ganga, Magnetic field effect on second order slip flow of nanofluid over a stretching/shrinking sheet with thermal radiation effect, J. Magn. Magn. Mater. 381 (2015) 243-257.

[9] P.S.N. Reddy, Ali J Chamkha, Soret and Dufour effects on MHD convective flow of Al_2O_3–water and TiO_2–water nanofluids past a stretching sheet in porous media with heat generation/absorption, Adv. Powder. Technol., 27(4) (2016) 1207-1218 .

[10] P.S. N. Reddy, Ali J Chamkha, Influence of size, shape, type of nanoparticles, type and temperature of the base fluid on natural convection MHD of nanofluids, Alexandria Engineering Journal, 55(1) (2016) 331-341.

[11] M. Ghalambaz, M.A. Sheremet, I. Pop, Free Convection in a Parallelogrammic Porous Cavity Filled with a Nanofluid Using Tiwari and Das' Nanofluid Model, PLoS One, 10(5) (2015) e0126486.

[12] F. Shahzad, Rizwan Ul Haq, Qasem M Al-Mdallal, Water driven Cu nanoparticles between two concentric ducts with oscillatory pressure gradient, J Mol Liq., 224 (2016) 332.

[13] M. Ghalambaz, A. Doostani, E. Izadpanahi, A.J. Chamkha, Phase-change heat transfer in a cavity heated from below: The effect of utilizing single or hybrid nanoparticles as additives, J Taiwan Inst Chem Eng, 72 (2017) 104-115.

[14] A.J. Chamkha, A. Doostanidezfuli, E. Izadpanahi, M. Ghalambaz, Phase-change heat transfer of single/hybrid nanoparticles-enhanced phase-change materials over a heated horizontal cylinder confined in a square cavity, Adv. Powder Technol. ,28 (2) (2017) 385-397.

[15] M. Ghalambaz, A. Doostanidezfuli, H. Zargartalebi Ali J. Chamkha, MHD phase change heat transfer in an inclined enclosure: Effect of a magnetic field and cavity inclination, Numer Heat Tr A Appl, 71 (1) (2017) 91-109.

[16] M. Ghalambaz, A. Doostani, Ali J. Chamkha, M. A. Ismael, Melting of nanoparticles- enhanced phase-change materials in an enclosure: Effect of hybrid nanoparticles, International Journal of Mechanical Sciences 134 (2017) 85-97.

[17] Rashid, Rizwan Ul Haq, Z.H. Khan, Qasem M Al-Mdallal, Flow of water based alumina and copper nanoparticles along a moving surface with variable temperature, , J Mol Liq., 246 (2017) 354-362.

[18] I. Rashid, Rizwan Ul Haq, Qasem M Al-Mdallal, Aligned magnetic field effects on water based metallic nanoparticles over a stretching sheet with PST and thermal radiation effects, Physica E Low Dimens Syst Nanostruct., 89 (2017) 33-42

[19] P. Besthapu, Rizwan Ul Haq, S. Bandari, Qasem M Al-Mdallal, Mixed convection flow of thermally stratified MHD nanofluid over an exponentially stretching surface with viscous dissipation effect, J Taiwan Inst Chem Eng, 71 (2017) 307-314.

[20] P.S. N. Reddy, Ali J Chamkha, Ali Al-Mudhaf, MHD heat and mass transfer flow of a nanofluid over an inclined vertical porous plate with radiation and heat generation/absorption, Adv. Powder. Technol., 28(3) (2017) 1008-1017 .

[21] Kh. Hosseinzadeh, A.Jafarian Amiri, S.Saedi Ardahaie, D.D.Ganji, Effect of variable lorentz forces on nanofluid flow in movable parallel plates utilizing analytical method, Case Studies in Thermal Engineering, 10 (2017) 595- 610.

[22] F. A. Soomro, R. Ul Haq, Qasem M Al-Mdallal, Q. Zhang, Heat generation/absorption and nonlinear radiation effects on stagnation point flow of nanofluid along a moving surface, Results in Physics, 8 (2018) 404-414.

[23] S. E. B. Maiga, C.T Nguyen, N. Galanis, G. Roy, Heat transfer behaviours of nanofluids in a uniformly heated tube, Superlattice .Microst., 35 (2004a) 543-557.

[24] S.E.B. Maiga, C.T. Nguyen, N. Galanis, G. Roy Heat transfer enhancement in forced convection laminar tube flow by using nanofluids. In: Proc. CHT-04 ICHMT Int. Symposium Advances Computational Heat Transfer, April 19-24 Norway, Paper No. CHT-04-101, (2004b)

[25] S.E.B. Maiga , S. J. Palm, C. T. Nguyen, G. Roy, N. Galanis, Heat transfer enhancement by using nanofluids in forced convection flows. Int. J. Heat Fluid Flow., 26 (2005) 530-546.

[26] C.V. Pop, S. Fohanno, G. Polidori, C.T. Nguyen, Analysis of laminar-to- turbulent threshold with water γ Al_2O_3 and ethylene glycol- γ Al_2O_3 nanofluids in free convection, Proceedings of the 5th IASME/WSEAS Int. Conference on heat transfer, thermal engineering and environment, Athens, Greece, August 25-27, 188 (2007)

[27] B. Farajollahi, S. Gh Etemad, M. Hojjat, Heat transfer of nanofluids in a shell and tube heat exchanger, Int. J. Heat Mass Transfer, 53 (2010) 12-17.

[28] T. M. O. Sow, S. Halelfadl, S., Lebourlout, C.T. Nguyen, Experimental Study of the Freezing Point of γ- Al_2O_3 Water Nanofluid. Advances in Mechanical Engineering, Article ID 162961 (2012)

[29] H. Beiki, M.N. Esfahany , N. Etesami, Laminar forced convective mass transfer of γ-Al_2O_3/electrolyte nanofluid in a circular tube, Int. J. Thermal Sciences., 64 (2013) 251-256 .

[30] E. Esmaeilzadeh, H. Almohammadi, A. Nokhosteen, A. Motezaker, A.N. Omrani, Study on heat transfer and friction factor characteristics of γ-Al_2O_3/water through circular tube with twisted tape inserts with different thicknesses. Int. J. Thermal Sciences., 82 (2014) 72-83.

[31] M. Abdul-Aziz, Azza H. Ali, H. Elkhatib, S.H. Othman, Effect of operating parameters on the transient behavior of gravity-assisted heat-pipe using radio- chemically prepared γ Al_2O_3 nano-fluid, Adv. Powder. Technol., 27 (2016) 1651-1662.

[32] A.M. Bayomy, M.A. Saghir, Experimental study of using γ-Al_2O_3–water nanofluid flow through aluminum foam heat sink: Comparison with numerical approach, Int. J. Heat Mass Tranfer, 107 (2017) 181-203.

[33] H. S. Moghaieb, H.M. Abdel-Hamid, M. H. Shedid, A.B. Helali, Engine Cooling Using γAl2O3/Water Nanofluids, Appl. Therm. Eng, (2016) http://dx.doi.org/10.1016/j.applthermaleng.2016.12.099

[34] N. Vishnu Ganesh, A.K. Abdul Hakeem, B. Ganga, A comparative theoretical study on Al_2O_3 and γ-Al_2O_3 nanoparticles with different base fluids over a stretching sheet, Adv. Powder. Technol., 27(2) (2016) 436–441.

[35] M.M. Rashidi, N. Vishnu Ganesh, A.K. Abdul Hakeem, B. Ganga, G. Lorenzini, Influences of an effective Prandtl number model on nano boundary layer flow of γ Al_2O_3–H_2O and γ Al_2O_3–$C_2H_6O_2$ over a vertical stretching sheet, Int. J. Heat Mass Transfer., 98 (2016) 616–623.

[36] Y. Lin, B. Li, L. Zheng, G. Chen, Particle shape and radiation effects on Marangoni boundary layer flow and heat transfer of copper-water nanofluid driven by an exponential temperature, Powder Technol., 301 (2016) 379-386.

[37] E. H. Aly, A. Ebaid, Exact analysis for the effect of heat transfer on MHD and radiation Marangoni boundary layer nanofluid flow past a surface embedded in a porous medium, J. Mol. liq., 215 (2016) 625–639.

[38] Y. Lin, L. Zheng, X. Zhang, Radiation effects on Marangoni convection flow and heat transfer in pseudo-plastic non-Newtonian nanofluids with variable thermal conductivity, Int. J. Heat Mass Transfer., 77 (2014) 708–716.

[39] T. Hayat, M. Ijaz Khan, M. Farooq, A. Alsaedi, T. Yasmeen, Impact of Marangoni convection in the flow of carbon–water nanofluid with thermal radiation, Int. J. Heat Mass Transfer, 106 (2017) 810–815.

[40] M. Sheikholeslami, A.J. Chamkha, Influence of Lorentz forces on nanofluid forced convection considering Marangoni convection, J. Mol. liq., 225 (2017) 750-757.

[41] S. Lee, S.U.-S. Choi, S. Li, J.A. Eastman, Measuring thermal conductivity of fluids containing oxide nanoparticles. J. Heat Transfer., 121 (1999) 280-289.

[42] X. Wang, X. Xu, S.U.-S. Choi, Thermal conductivity of nanoparticles-fluid mixture, J. Thermophys. Heat Transfer, 13 (4) (1999) 474-480.

[43] H. Masuda, A. Ebata, K. Teramae, N. Hishinuma, Alteration of thermal conductivity and viscosity of liquid by dispersing ultrafine particles , Netsu Bussei., 4 (4) 227-233 (1993)

[44] R.L. Hamilton, O.K. Crosser, Thermal conductivity of heterogeneous two-component systems. I and EC Fundamentals, 1 (3) (1962)187-191.

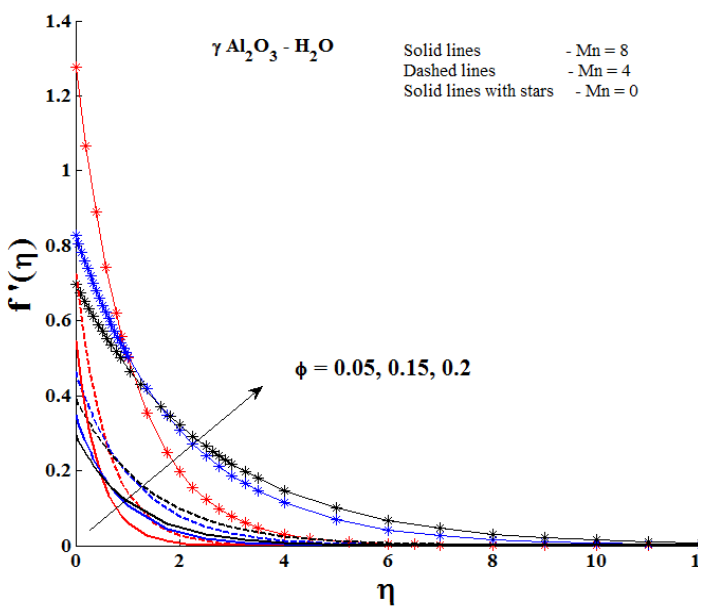

1. (a)

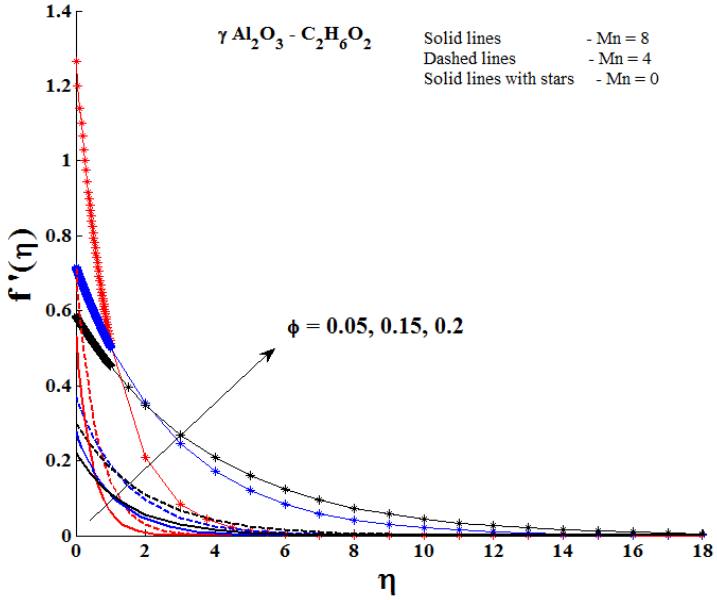

1. (b)

Fig. 1. Combined effect of nanoparticle volume fraction (ϕ) and magnetic parameter (Mn) on velocity profile with Rd= 2 and θ_w = 1.5 (a) γ Al_2O_3 – H_2O with Pr = 6.96 (b) γ Al_2O_3 – $C_2H_6O_2$ with Pr=204 .

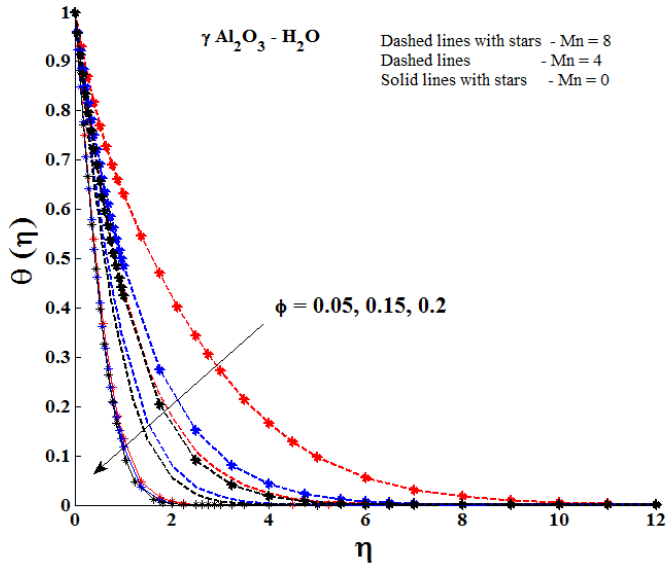

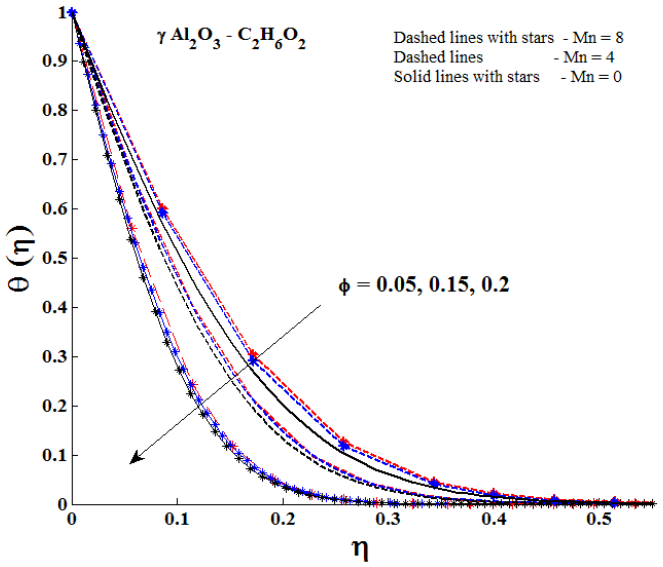

2. (a) **2. (b)**

Fig. 2. Combined effect of nanoparticle volume fraction (ϕ) and magnetic parameter (Mn) on temperature profile with Rd= 2 and θ_w = 1.5 (a) γ Al_2O_3 – H_2O with Pr = 6.96 (b) γ Al_2O_3 – $C_2H_6O_2$ with Pr=204 .

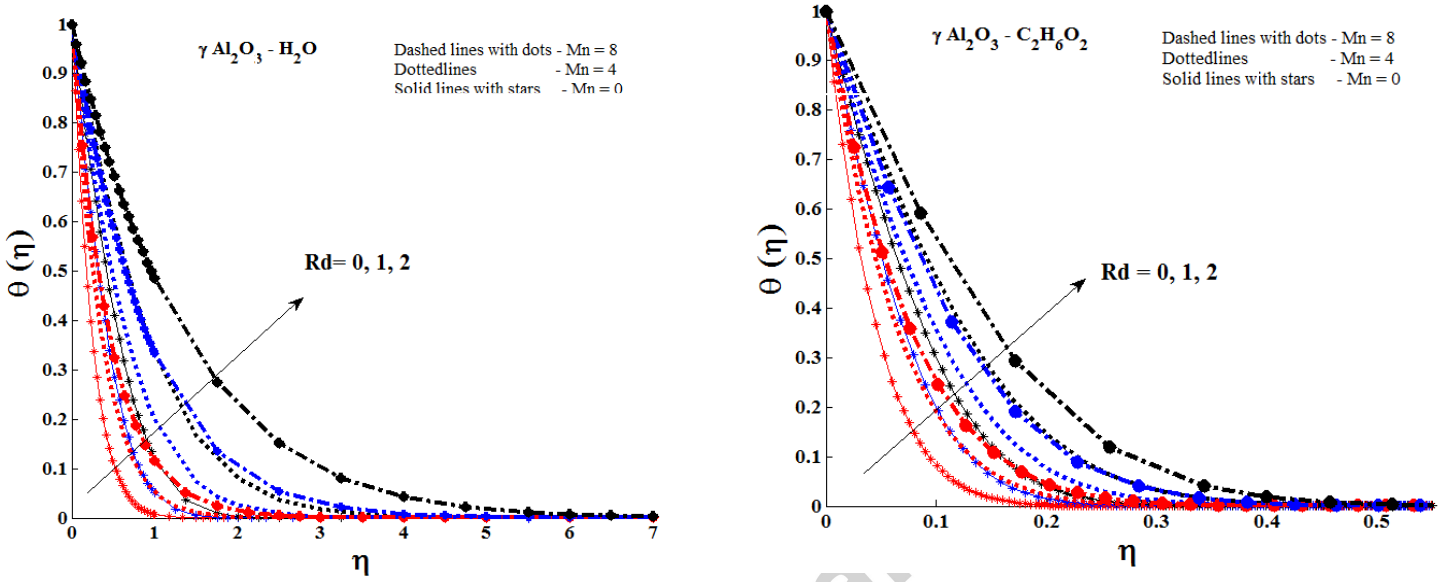

3. (a) **3. (b)**

Fig. 3. Combined effect of radiation parameter (Rd) and magnetic parameter (Mn) on temperature profile with ϕ= 0.15 and θ_w = 1.5 (a) γ Al_2O_3 – H_2O with Pr = 6.96 (b) γ Al_2O_3 – $C_2H_6O_2$ with Pr=204 .

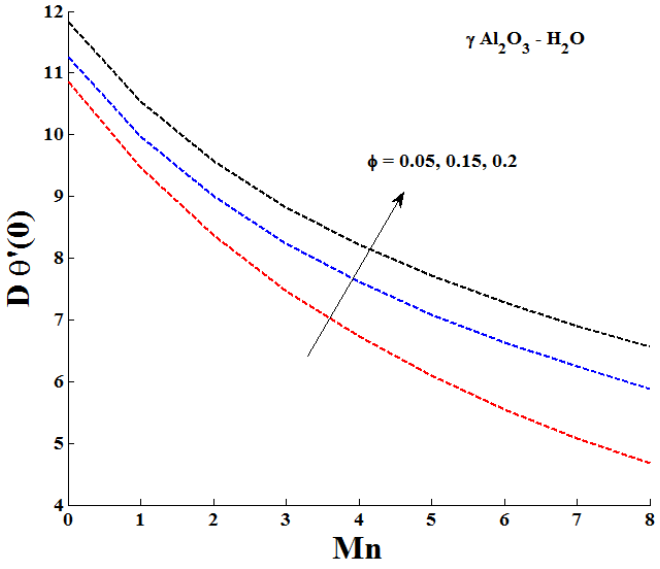

4. (a)

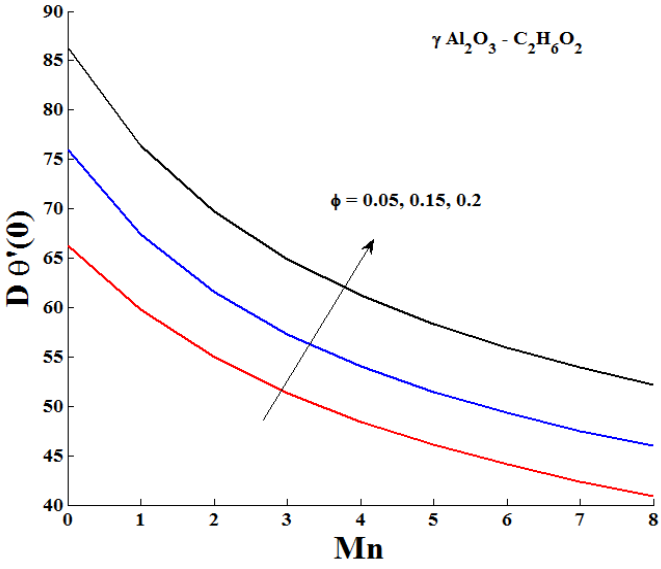

4. (b)

Fig. 4. Combined effect of nanoparticle volume fraction (ϕ) and magnetic parameter (Mn) on reduced Nusselt number with Rd= 2 and θ_w = 1.5 (a) γ Al_2O_3 – H_2O with Pr = 6.96 (b) γ Al_2O_3 – $C_2H_6O_2$ with Pr=204 .

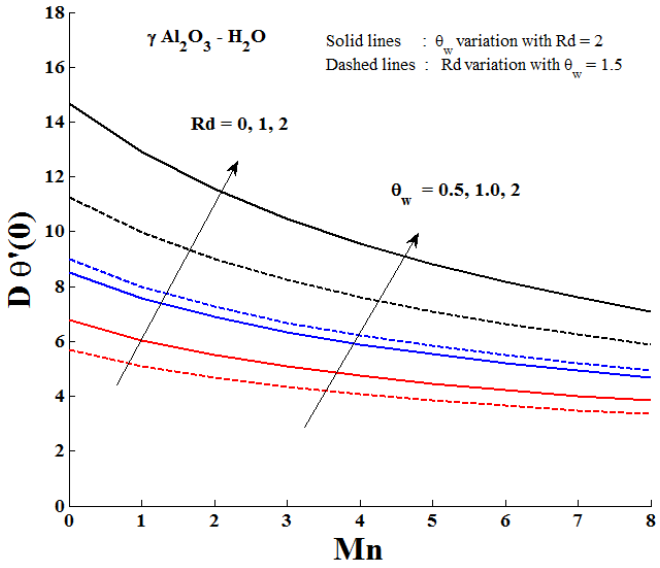

5. (a)

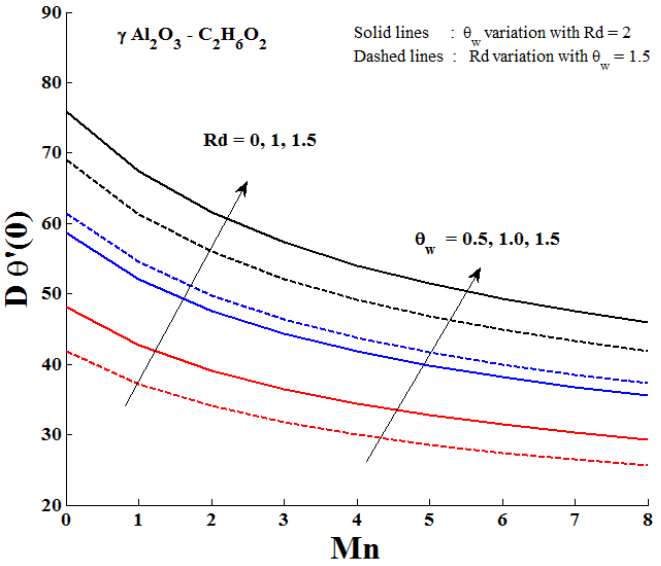

5. (b)

Fig. 5. Combined effect of radiation (Rd), temperature ratio (θ_w) and magnetic parameters (Mn) on reduced Nusselt number with ϕ=0.15 (a) γ Al_2O_3 – H_2O with Pr = 6.96 (b) γ Al_2O_3 – $C_2H_6O_2$ with Pr=204 .

Table 1.Thermo-physical properties of water, ethylene glycol and alumina [21]

	ρ (kg/m^3)	C_p (J/kg K)	k(W/m K)	σ (Ω. m)$^{-1}$	Pr
Pure water (H_2O)	998.3	4182	0.60	0.05	6.96
Ethylene glycol ($C_2H_6O_2$)	1116.6	2382	0.249	1.07×10^{-7}	204
Alumina (Al_2O_3)	3970	765	40	10^{-12}	-

Highlights

- Magnetic field effect on γ Al_2O_3 nanoparticles investigated first time.
- Maragoni boundary layer flow along with non –linear thermal radiation considered.
- Water and Ethylene glycol are taken as base fluids.
- The experimental based thermo physical properties are used.
- Results discussed for γAl_2O_3 nanoparticles with an effective Prandtl number model.

.